Recommended Procedures for Damage-Based Serviceability Design of Steel Buildings under Wind Loads

KEVIN ASWEGAN, FINLEY A. CHARNEY and JORDAN JARRETT

ABSTRACT

This paper provides a recommended procedure for nonstructural damage control of steel buildings under serviceability-level wind loads. Unlike traditional procedures that provide a single drift limit under a given reference load, the recommended procedure provides a decision space that spans a range of wind hazards and associated damage states. Central to the procedure are the use of shear strain in nonstructural components as the engineering demand parameter and the use of component fragility as a reference for limiting damage.

Keywords: wind, drift, serviceability, damage, fragility, performance-based engineering.

BACKGROUND

During the design of a building, the structural engineer is typically concerned with both strength and serviceability limit states. Design and detailing requirements for the strength limit states such as yielding, fracture and buckling are prescribed in the applicable building codes. However, the same building codes do not provide prescriptive requirements for the serviceability limit states. This is largely due to the noncatastrophic nature of serviceability failures, as well as the fact that serviceability issues are generally specific to a project and thus require participation from the project owner and other design team members.

Instead of providing serviceability requirements, the codes take a performance-based approach wherein only the expectations of a successful design are provided. The AISC *Specification* (AISC, 2010) defines serviceability as "a state in which the function of a building, its appearance, maintenance, durability and comfort of its occupants are preserved under normal usage." On the topic of drift, the specification states that drift "shall be evaluated under service loads to provide for serviceability of the structure, including the integrity of interior partitions and exterior cladding." ASCE 7-10 (ASCE, 2010) contains similar language, stating that "sufficient stiffness must be provided such that deflection, drift, and vibrations are limited to an acceptable level."

The lack of wind serviceability design standards has led to a wide variation in design practices across the United States. To assess the state of the practice, ASCE created the Task Committee on Drift Control of Steel Building Structures in 1984. The committee surveyed structural engineering firms and released its results in 1988 (ASCE, 1988). In general, the results from the survey showed that there was little consistency in terms of the selection of service-level wind loads, the development of mathematical models of the structural system, the selection of appropriate drift measures and the establishment of drift limits. A more recent survey, conducted in 2006 by the ASCE/SEI Committee on the Design of Steel Building Structures, found similar results (Charney and Berding, 2007). When asked to list the primary motivation for limiting drift, the respondents to the most recent survey reported, in the following order: to prevent structural damage (most common response), to prevent nonstructural damage, to control second-order (P-Δ) effects, and to limit lateral accelerations. With the possible exception of P-Δ effects (which contribute to drift), these motivations are all serviceability considerations.

One approach to improving wind drift serviceability design would be to borrow from the concepts of performance-based earthquake engineering, commonly referred to as PBEE, that are already in use for existing buildings through the provisions of ASCE 41-13 (ASCE, 2013) and that have been recommended for tall buildings (PEERC, 2010). The PBEE concept is built around quantifying hazard intensity measures, engineering demand parameters, damage measures and decision variables (repair cost, repair time or casualties) at multiple limit states. In order to account for inherent uncertainties in the process, the PBEE methodology

Kevin Aswegan, Structural Engineer, Magnusson Klemencic Associates, Seattle, WA. Email: kaswegan@mka.com

Finley A. Charney, Ph.D., P.E. Professor of Structural Engineering, Department of Civil Engineering, Virginia Tech, Blacksburg, VA (corresponding). Email: fcharney@vt.edu

Jordan Jarrett, Structural Engineering Graduate Student, Department of Civil Engineering, Virginia Tech, Blacksburg, VA. Email: jaj14@vt.edu

Paper No. 2013-14

is supported by a probabilistic framework (Moehle and Deierlein, 2004). Various government supported efforts to develop a comprehensive PBEE procedure recently cumulated with the publication of the FEMA P-58 report (FEMA, 2013a) and related materials, including a performance assessment calculation tool.

The development and advancement of performance based wind engineering (PBWE) would logically follow closely that of PBEE. However, there are significant differences related to the wind and seismic hazards, the limit states that need to be considered and the necessity (in seismic design) to explicitly include inelastic behavior associated with life-safety and collapse-prevention limit states. Paulotto, Ciampoli and Augusti (2004), Ciampoli, Petrine and Augusti (2011), and Griffis et al. (2012) proposed the adaptation of the PBEE framework to wind. Paulotto et al. and Ciampoli et al. provide probabilistic frameworks that incorporate the concepts of fragility. Fragility is also central to the FEMA P-58 PBEE procedure, as well as the procedure recommended in this paper. Griffis et al. propose multiple wind-related performance levels, dynamic nonlinear analysis of structures under wind loading and the concept of allowing inelastic behavior at more severe wind limit states. Despite the various proposals, without a coordinated government-supported effort to develop PBWE, it has not gained, nor is it likely to achieve, the same level of usage as PBEE.

The purpose of this paper is to describe a damage-based method for the evaluation and design of steel structures subjected to serviceability-level wind loads. While the proposed method falls short of PBWE as envisioned by the authors cited earlier, it does address three key issues: selection of appropriate wind loads, accurate definition and calculation of the damage measure and selection of rational damage limits. Unlike other methodologies that rely on a single wind return period or a set of established drift limits, the procedure described in the remainder of this paper follows the basic principles on serviceability that were published in 1986 (Committee on Serviceability, 1986), which states:

> *Serviceability guidelines need to be flexible and adapt*able *to different occupancies, use requirements and techniques for integrating nonstructural components. The guidelines ought to be negotiable, within limits, between the engineer, architect and building owner.*

OVERVIEW OF PROCEDURE

The procedure is based on the computation and limitation of shear deformations in nonstructural components. Features of the procedure, described in much more detail later, are as follows:

1. The procedure is developed explicitly for the serviceability assessment of tier-type structures (a structure in which levels are stacked on one another or built in tiers). This limitation is applicable because such buildings have numerous interior architectural partitions and exterior finishes that need to be protected from damage.

2. A broad wind-hazard basis is used, wherein a range of mean recurrence intervals are considered.

3. The deformation that is controlled is shear strain in nonstructural components.

4. A three-dimensional mathematical model of the building is used to perform the structural analysis and is calibrated to provide the best possible estimate of the damaging shear strain deformations in the nonstructural components. A different model would likely be used to address strength limit states.

5. The limiting shear strain is based on the concept of structural fragility and the use of fragility curves. Such curves are based on laboratory testing of nonstructural components and provide the probability of exceeding a given damage state (e.g., minor cracking of drywall partitions) given the computed shear strain.

6. The results of the serviceability analysis provide a broad basis for making decisions about controlling damage in nonstructural components but fall short of providing quantitative information on the consequences of accepting some damage.

While the procedure could be expanded to consider other wind-related serviceability limit states—such as perception of motion—and to include structural damage, the current focus is on the control of damage in nonstructural components, such as interior walls and exterior walls and finishes. Damage under seismic loads could also be controlled using the same general procedure.

WIND LOADS

Current Wind Load Design Provisions

Buildings in the United States are designed for wind loads according to the provisions of ASCE 7. The current edition, ASCE 7-10 (ASCE, 2010), provides three methods for determining wind loads for the main wind-force resisting system of a building: the directional procedure, the envelope procedure and the wind tunnel procedure. The wind tunnel procedure is generally the most accurate but also the most time-consuming and expensive. For the serviceability-level wind loads, any of the allowed procedures are suitable, provided that an appropriate mean recurrence interval (MRI) is selected.

Mean Recurrence Interval (MRI)

The mean recurrence interval is the return period for a wind event. A 10-year MRI refers to a wind event that occurs, on average, once every 10 years. A shorter MRI corresponds to lower-intensity wind loads, while a longer MRI corresponds to higher-intensity wind loads. For risk category II buildings designed according to the provisions of ASCE 7-10, the MRI is 700 years. Risk category I and III–IV buildings are designed using 300- and 1700-year MRIs, respectively. Each of these risk-related MRIs represents ultimate strength-level loading, and as such, the load factor on wind loads is 1.0. Service-level wind speeds (as used in previous editions of ASCE 7) are generally in the range of 50 to 100 years. The wind loads based on these service-level wind speeds must be factored up to strength level for the design of the main lateral load-resisting system. Similarly, the service-level wind speeds are generally factored down for serviceability considerations. It is important to note that "service"-level wind speeds and "serviceability" are not synonymous. It was never the intent in ASCE 7 to use service-level loads for serviceability.

Various authors have recognized that the service-level and, particularly, the ultimate-level wind loads are overly conservative for serviceability considerations when traditional drift limits (in the range of $H/500$, where H is the story height) are used. For this reason, Tallin and Ellingwood (1984), Charney (1990b), and Griffis (1993) proposed serviceability MRIs of 8 to 10 years. This particular MRI range is approximately the length of the average tenancy in the United States and the United Kingdom (Ellingwood and Culver, 1977). Additionally, AISC *Design Guide 3* (West, Fisher and Griffis, 2003) recommends a 10-year wind event for interstory drift checks.

Although many sources have suggested a 10-year MRI, it is recommended that a designer select a wind serviceability MRI based on the specific needs of the owner or other stakeholders relative to the use (risk category) of the building and the probability of and potential consequences of exceeding a particular damage limit state. Another factor in determining the appropriate MRI is the range and resolution of test data have has been used to establish damage limits. This important concept is discussed later in the paper in association with the use of component fragility as a damage indicator.

Recognizing the need to use a lower MRI for serviceability considerations, the commentary to Appendix C of ASCE 7-10 provides wind speed maps for 10-, 25-, 50- and 100-year MRIs. Using the 10-, 25-, 50- and 100-year wind speed maps, a designer can select the appropriate wind speed and use the provisions of ASCE 7 to determine the serviceability wind loads. When a building site is located such that it is difficult to manually determine the wind speed with the ASCE 7 maps, an online tool developed by the Applied Technology Council (ATC, 2013) can be used. This tool, using the same data that was used to generate the ASCE 7 maps, will provide wind speeds for various MRIs given a physical address or latitude and longitude.

Wind and Seismic Hazard Curves

A hazard curve is a plot showing the relationship between a hazard measure (such as wind speed or wind pressure) and likelihood of occurrence. Figure 1 shows wind hazard curves for select cities across the United States. The vertical axis shows the velocity pressure (q_z in ASCE 7-10), assuming that the wind directionality factor (K_d), the velocity pressure exposure coefficient (K_z) and the topographic factor (K_{zt}) are each equal to 1.0. The likelihood of occurrence is represented by MRI on the horizontal axis.

The wind hazard curves contain valuable information relating to service and ultimate level wind loads. For the 10-year MRI, the wind pressures are similar for the six cities shown, varying between 13.3 and 16.0 psf. Examining the wind pressures for one particular MRI, however, can be misleading. For example, in the cities of Charleston and Memphis, the wind pressures due to the 10-year MRI are equal (14.8 psf). This is not the case, however, for higher MRIs. For the 700-year MRI (ultimate-level wind loads), the wind pressure in Charleston significantly diverges from the wind pressure in Memphis. The difference is due to the fact that Charleston is located in the hurricane region of the United States. It should also be noted that due to the location of Charleston, New Orleans, and Boston along the hurricane-prone coast, where the mapped wind speed contours are tightly spaced, seemingly small changes in latitude or longitude between locations can lead to significant differences in speeds and wind pressures.

It is of some interest to compare the wind and seismic hazards, as well as to discuss the MRIs typically used for seismic serviceability. Figure 2 presents seismic hazard curves for the same six U.S. cities shown in Figure 1. These curves show 5% damped, site class B–C boundary, 1-s spectral acceleration, plotted against MRI.

While the shapes of the wind hazard curves are similar for the cities indicated, the shapes of the seismic hazard curves are quite different. The difference is most noticeable when one distinguishes between Pacific west coast and the central and eastern U.S. locations. For example, in Charleston, the 50-year spectral acceleration is only 4.5% of the 500-year value, while in San Francisco, the 50-year acceleration value is much higher at 28% of the 500-year spectral acceleration. A general conclusion from the wind and the seismic hazard curves is that seismic serviceability is not likely to be a controlling issue in the central and eastern United States and that wind serviceability is probably not a controlling issue along the Pacific west coast (except for tall buildings, where perception of motion can become a controlling design consideration).

In performance-based earthquake engineering, serviceability-level drifts are determined for events with an MRI in the range of 43 years (PEERC, 2010) to 72 years (ICC, 2012). The data to assess seismic hazard at MRIs shorter than 43 years is generally not available. It is also important to note that nonstructural and some degree of structural damage (including minor yielding of steel) is *expected* under the 43- to 72-year shaking in the western United States. For example, the Pacific Earthquake Engineering Research Center (PEERC) Tall Building Guidelines limit interstory drift to 0.5% of the story height (*H*/200) when the structure is subjected to the 43-year MRI. Other seismic serviceability drift limits are summarized by Dymiotis-Wellington and Vlachaki (2004).

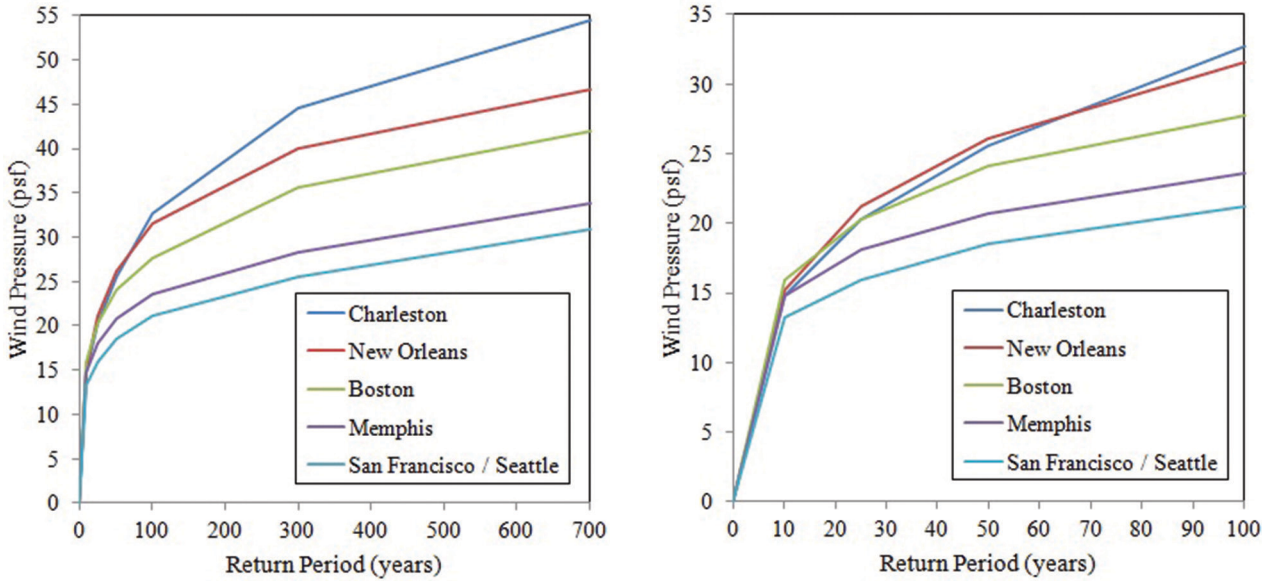

Fig. 1. Wind hazard curves for select U.S. cities: (a) return periods between 0 and 700 years; (b) return periods between 0 and 100 years.

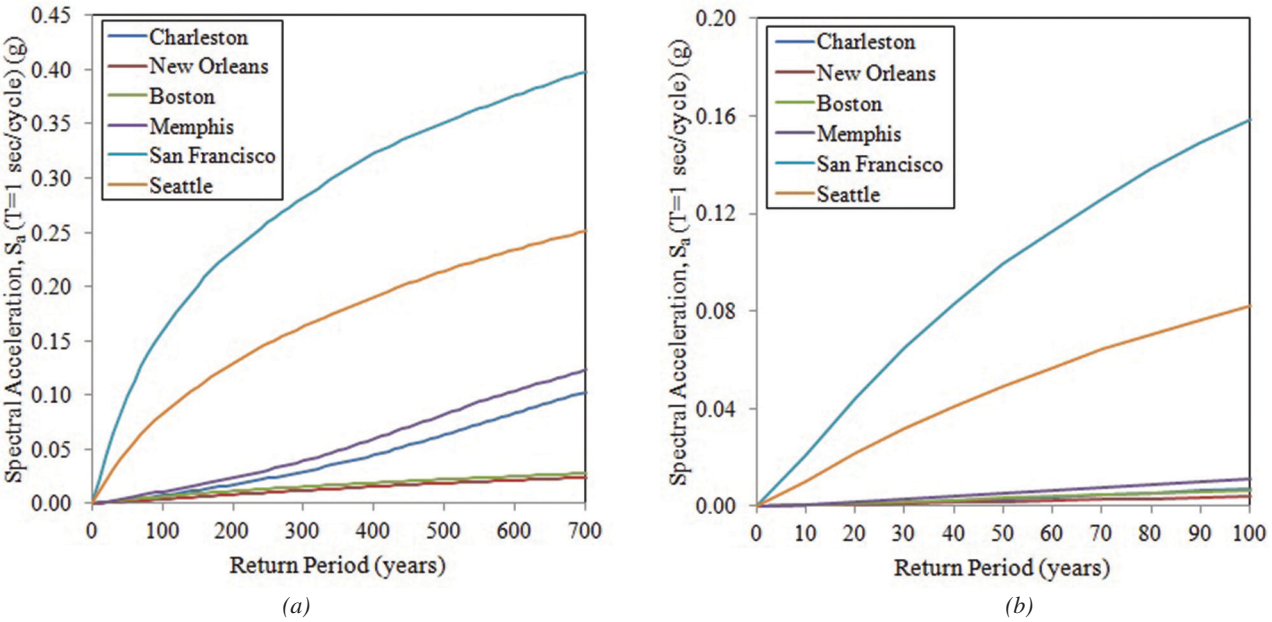

Fig. 2. Seismic hazard curves for select U.S. cities: (a) return periods between 0 and 700 years; (b) return periods between 0 and 100 years.

For wind-based serviceability, MRIs in the range of 10 to 50 years are appropriate because it is in this range of wind loads that nonstructural components will first experience damage. As described later, it is recommended that a 25-year MRI be used as the basic wind speed for wind damage serviceability because it is in this range of loading that the test-based fragility data are likely to be most reliable. Deformation demands for different wind MRIs can be estimated from those determined by the 25-year MRI as follows:

$$\delta_{Mx} = \delta_{M25} \frac{V_{Mx}^2 G_{Mx}}{V_{M25}^2 G_{M25}} \quad (1)$$

where δ_{Mx} is the deformation demand under an x-year MRI wind, δ_{M25} is the same deformation demand under the 25-year MRI wind, V is the basic wind velocity and G is the gust factor for the indicated MRIs. The gust factors are computed in accordance with Section 26.9 of ASCE 7-10. Torsional effects are calculated by applying the ASCE 7 design wind loads cases, which require 75% of the load be applied at an eccentricity of 15% of the width of the building.

PREDICTING DAMAGE IN STRUCTURES

Drift as a Damage Measure

Given that the purpose of the serviceability analysis is to prevent or control damage, the response quantity used to predict damage and the associated damage limits must be consistent with the physical mechanism that causes damage. Borrowing from the field of performance-based earthquake engineering, the following terms are used in this paper:

- ***Engineering demand parameter*** (EDP) is the computed quantity that is used as a predictor of damage. Traditional serviceability analysis uses interstory drift as the EDP. The procedure presented herein uses shear strain as the EDP.
- ***Damage state*** (DS) is a physical description of the expected damage. An example is first observation of cracking in a brick masonry veneer.
- ***Damage measure*** (DM) is the value of the EDP at which a certain damage is expected to occur. Traditional serviceability analysis used an interstory drift limit as the DM. The procedure outlined in this paper does not provide a specific limit and, instead, uses fragility curves to estimate the probability of exceeding a given damage state.

The concept of the EDP is discussed in this section of the paper. The damage measure and damage states are discussed in later sections.

Traditional EDPs include total drift, roof drift, and interstory drift (and, for other applications, floor acceleration and plastic hinge rotations are also used). Total drift is the lateral displacement of a frame at a given level with respect to a chosen datum (typically the ground). Roof drift is simply the total drift measured at the roof level. Interstory drift is the relative lateral displacement between two adjacent levels. Note that throughout this paper the term *interstory drift* is used, although the term *story drift* would also be appropriate. The drift index is the total, roof or interstory drift divided by the height over which the drift applies. For example, the interstory drift index (IDI) is the interstory drift divided by the height of the story. This same quantity is also referred to as the interstory drift ratio. Based on the surveys cited earlier, most engineers attempt to control drift by providing limiting values on the computed interstory drift or the interstory drift ratio.

The interstory drift and the interstory drift ratio are not, however, accurate measures of damage in a nonstructural component and are, therefore, not the most suitable EDPs if the purpose of the analysis is to limit damage in the nonstructural components. This is because interstory drift tracks only lateral displacement (not necessarily equal to deformation) and does not account for vertical racking or rigid-body rotation. A true damage measure for nonstructural components, accounting for both horizontal and vertical racking but excluding rigid-body rotation, would be mathematically equivalent to the in-plane shear strain in the component.

Another reason for using shear strain as the EDP is that it is the best quantity to correlate with laboratory tests on nonstructural components. These tests are typically performed by loading the specimens in pure shear and then correlating the damage, as it occurs, to the shear strain imposed on the specimen at the time the damage is observed. As described later in this paper, the same laboratory tests may produce sufficient information to establish the fragility of the tested component. The use of fragility in wind damage serviceability analysis allows the engineer not only to establish damage limits, but also to determine the probability that damage will occur if the imposed limits are reached or exceeded.

Using Shear Strain as the Engineering Demand Parameter

To alleviate the shortcoming of interstory drift as a damage measure, Charney (1990b) developed a revised damage measure, called the drift damage index, which in this paper is renamed the deformation damage index (DDI) to eliminate the reliance on horizontal drift as a damage measure. In accordance with the terminology adopted in the previous section, the DDI can be used as the EDP for the proposed method. The DDI is mathematically equal to the shear strain in a vertical rectangular panel of the structure, called a drift damageable zone, here renamed a deformation damageable

zone (DDZ). A DDZ spans between floors in the vertical direction and between column lines (real or imaginary) in the horizontal direction. For two-dimensional analysis, only the horizontal and vertical displacements are needed at the four corners (nodes) of the DDZ. For three-dimensional analysis, the two horizontal displacement components would need to be transformed into the plane of the DDZ. As shown later, this procedure can be automated by the use of special finite elements, called *damage gages*.

Conceptually, the DDZ can represent interior, nonstructural partitions (such as a gypsum wall), exterior walls or any other damageable element in a building model. When a building model is created and loaded with the appropriate wind loads, each DDZ will have an associated DDI, defined by the following equation:

$$DDI = 0.5\left[\frac{X_A - X_C}{H} + \frac{X_B - X_D}{H} + \frac{Y_D - Y_C}{L} + \frac{Y_B - Y_A}{L}\right] \quad (2)$$

where X_N is the lateral deflection at node N, Y_N is the vertical deflection at node N, H is the story height and L is the width of the DDZ (usually the bay width). These variables are shown in Figure 3. Note that the terms in Equation 2 containing X-direction lateral deflection values represent the interstory drift index. If the terms representing vertical deflection were set to zero, the DDI would be equal to the IDI.

Damage Gages

Computation of the deformation damage index can be cumbersome, particularly for three-dimensional analysis. When using a finite element analysis program, the DDI can easily be computed by placing membrane or shell elements in the desired location. For example, the DDZ shown in Figure 3a can be represented by a four-node element. When specifying the properties of this element, it is necessary to use a very low thickness and/or modulus of elasticity such that the element does not significantly contribute to the stiffness of the structure. If a shear modulus of 1.0 is used, then the reported shear stress is identical to the shear strain, and thus the DDI is automatically determined. In general, it is preferable to average the shear strains at the four corners of the element to obtain the best estimate of the DDI. It is noted that when finite elements are used to represent the DDZ, the elements can be placed in any orientation, are not restricted to vertical planes and need not be rectangular in shape.

An example of the analysis of a 10-story X-braced planar frame is provided to clarify the concepts of computing DDIs using damage gages. This example will also be used later in

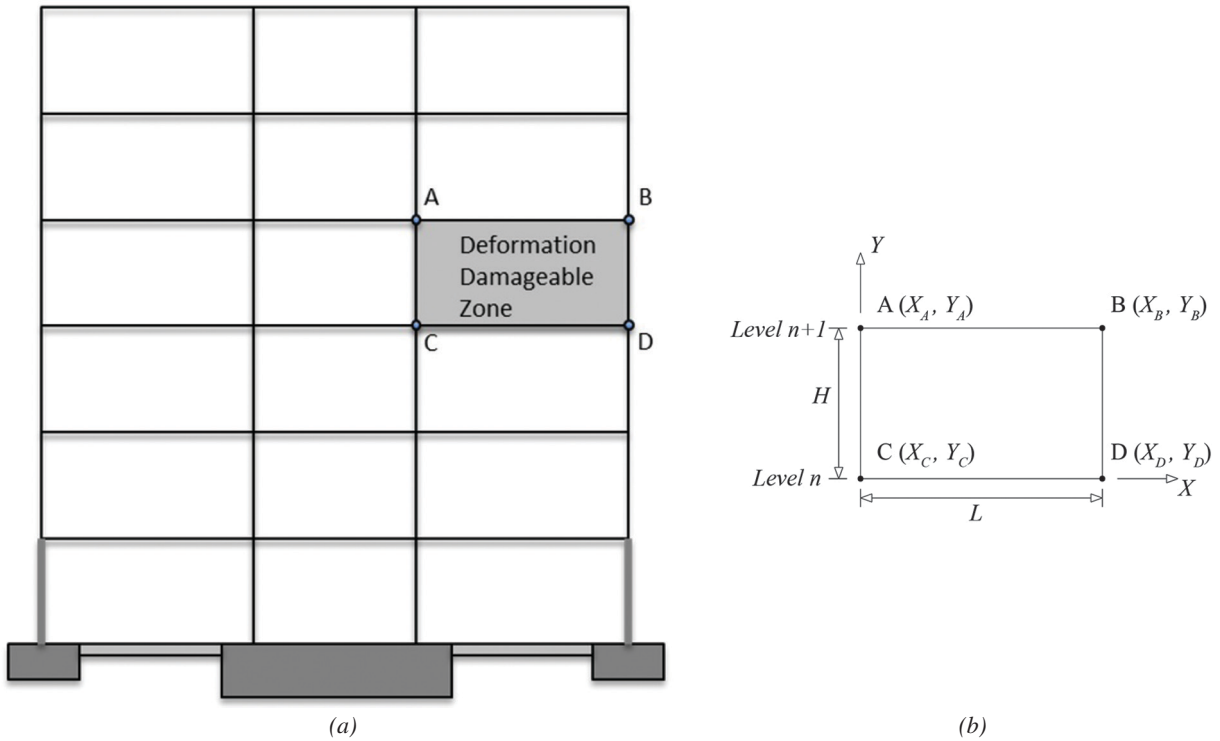

Fig. 3. Deformation damageable zone: (a) location in frame; (b) details for calculation.

Table 1. DDI Calculations for Top Left Bay in Example 1			
Node	**Lateral Displacement (ft)**	**Vertical Displacement (ft)**	**Shear Strain**
A	0.1920	0.0000	0.00315
B	0.1911	0.0270	0.00236
C	0.1686	0.0000	0.00315
D	0.1679	0.0267	0.00235
			DDI = 0.00275
			Average shear strain = 0.00275
			Conventional interstory drift index = 0.00186

the paper to demonstrate the use of fragility in wind damage analysis. A more detailed analysis of a 12-story building is provided in Appendix A.

The example frame has three 30-ft-wide bays, and the story height is constant at 12.5 ft. The building is located in Dallas, Texas, and is designed for the ultimate-level wind speeds for that location. The column sections are W14s, and the beams range from W24s to W30s. The lateral force resisting system is an X-braced frame in the center bays in which the members are W12s. For this example, a service-level wind loading corresponding to a 25-year MRI is applied to the structure. The 25-year MRI was selected due to the hypothetical owner's preference that the serviceability design be based on a 25-year time period.

The structure is modeled in SAP2000 (Computers and Structures Inc., 2009). All connections and column bases are modeled as pinned. To calculate the DDI, a damage gage (DG) shell element is inserted into each bay, representing an interior partition wall. The elements are connected to the frame only at the four corners of each bay. The shear modulus of the DG element is assigned a unit value so that the calculated shear stress in the element is numerically equal to the shear strain. After the shear strains have been calculated for the elements, the DDI will be equal to the average of the shear strain values at the four corners of the element.

The analysis is run for the applied loads, and the nodal displacements and DDIs in the elements are determined. Table 1 contains the displacements and shear strains for the top left bay of the structure. The DDI, average shear strain and conventional interstory drift index are calculated based on the values at the nodes. Figure 4 shows the 10-story braced frame with the applied loading. The shear strain contours are plotted on each element, with the DDI labeled at the center of the element and the conventional interstory drift index labeled in parentheses. Equation 2 can also be used to calculate the DDI given the calculated nodal displacements. However, for the example, the DDI for each bay is calculated by averaging the values of the shear strain at the corners of the element.

Some important observations can be made based on the results shown in Figure 4. The first is that the DDIs in the outer bays are very different than the DDIs in the inner bay, even for the same story. For example, the DDI in the top left bay is equal to 0.00275, while the DDI in the adjacent braced bay is 0.000071 (only 2.6% of the value for the unbraced bay), despite having nearly equal conventional interstory drift indices. This difference is present, but less pronounced, at lower levels as well. A second observation is that the DDIs are significantly different from the conventional interstory drift indices (which only account for horizontal racking). For the top left bay, the conventional interstory drift index is 0.00186, which is 68% of the DDI. In the adjacent braced bay, the conventional interstory drift index is 26 times the DDI. This wide discrepancy is due to the fact that the conventional interstory drift index does not include vertical racking and does not remove the influence of rigid-body rotation. For this example, the nodes comprising the inner braced bays experience significant vertical deflections, particularly in the upper stories.

STRUCTURAL MODELING

Accurate computation of the EDP requires a mathematical model that can account for any source of deformation that contributes to the EDP. Thus, *any part* of the building-foundation system that is stressed under the wind load should, theoretically, be included in the mathematical model. This includes components of the main lateral load-resisting system, components of the gravity load-resisting system, architectural components, diaphragms, the soil-foundation system and all connections. Additionally, second-order (P-Δ) effects should be included. For example, for steel moment frames, the modeling of the columns and (possibly composite) beams should allow for unrestricted axial, flexural, shear and torsional deformation. Additionally, deformations in the panel-zone of the beam-column joints should be considered.

The importance of including all appropriate deformation sources in the structural components was illustrated in a

study performed by Charney (1990a), which quantified the relative influence of the various deformation sources on the overall lateral deflection of a frame. Using the principle of virtual work and the concept of displacement participation factors (Charney, 1991; Charney, 1993), 45 different steel structures were analyzed, ranging from 10 to 50 stories. It was found that flexural deformations are very influential in shorter, stockier structures and that axial deformations are influential in taller slender structures. Shear deformations contributed, on average, 15.6% to the overall lateral deflection. Panel zone deformations were found to constitute an average of 30.5% of the drift in a structure. A study by Berding (2006) found similar results, with panel zone deformations comprising as much as 39% of the total deformation. Based on the results of these studies, it is recommended that any structural model used to calculate deformation include the effects of axial, flexural, shear and panel zone deformations. The exclusion of any of these effects could result in the underestimation of component deformations.

Given that most commercial programs are designed to develop 3D models of building structures, it is recommended that a 3D model be used for all wind damage serviceability analyses. There are several advantages to utilizing a 3D building model, such as modeling the interaction of orthogonal building frames, and the automatic inclusion of inherent torsional response. Torsion can increase the computed shear strain in some parts of a building, while decreasing the shear strain in others. The torsional response is difficult, if not impossible, to model in 2D.

Additional modeling considerations are briefly provided in the following sections. More detailed recommendations can be found in Berding (2006).

Panel Zone Deformations

As previously discussed, panel zone deformations can constitute a significant contribution to the overall drift of a steel moment-resisting frame. There are several methods to model panel zone deformations, including the clearspan model, the

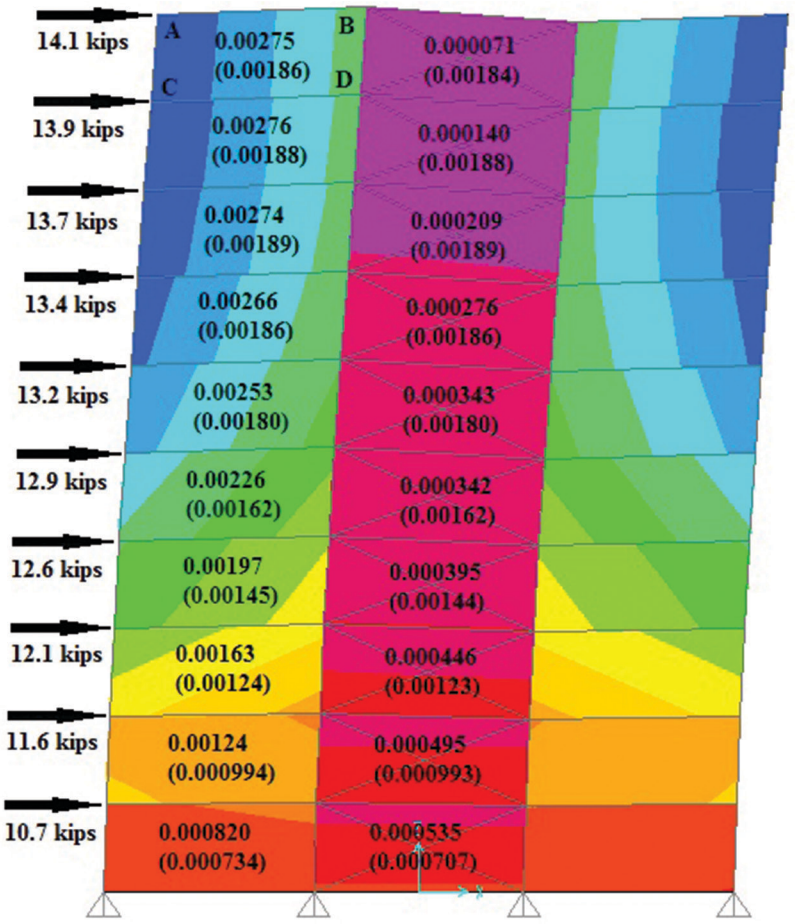

Fig. 4. Shear strains and (interstory drift indices) in a 10-story braced frame under serviceability-level wind loads.

centerline model, and more sophisticated mechanical joint models, such as the Krawinkler joint (KJ) and scissors joint (SJ) models (Charney and Marshall, 2006). The clearspan model unconservatively assumes the panel zone is infinitely rigid and should never be used. The centerline model uses center-to-center dimensions and will tend to overestimate flexural deformations and underestimate shear deformations within the beam-column joint. These effects partially offset each other, leading the centerline model to be sufficiently accurate in most situations (as long as there is no yielding in the panel zone). The KJ and SJ models are the most accurate and incorporate rigid links and rotational springs and explicitly represent both shear and flexural deformation within the beam-column joint. However, these models are somewhat difficult to implement. It is recommended that the centerline model be used when the mechanical joint models are not feasible (Charney and Pathak, 2008).

Floor and Roof Diaphragms

In most circumstances the floor and roof diaphragms may be modeled as rigid in their own plane and flexible out of plane. However, for certain structures, the out-of-plane stiffness of the diaphragms may act to couple the lateral load-resisting elements, thereby having a significant influence on lateral displacements and damage prediction.

Composite Beams

For serviceability analysis, it is generally acceptable to include some contribution from slabs, even if the beams are not designed as fully composite. The main concerns are related to the effective width of slabs to use in analysis and to the effectiveness of the slab if it is likely to be cracked in tension under serviceability wind loads. The slab can generally be broken into four moment regions under lateral loads (Schaffhausen and Wegmuller, 1977): (1) positive bending moment region—slab is located away from the column; (2) positive bending moment region—slab is adjacent to a column; (3) negative bending moment—slab is adjacent to interior column and may have compression reinforcement; and (4) negative bending moment region—slab is adjacent to exterior column and is not likely to have compression reinforcement. In general, for regions 1 and 2, the full effective slab width should be used. In a strict sense, the effective slab width should reduce to the width of the column for region 2. For regions 3 and 4, the girder properties alone should be used. In the determination of the composite moment of inertia for regions 1 and 2, the compressive strength of the concrete and the composite percentage based on the number of shear connectors should be considered. For a discussion on effective width, the reader is directed to Vallenilla and Bjorhovde (1985).

Gravity System

In some cases it may be worthwhile to include the additional lateral stiffness of the gravity system in the structural model. To do so, the engineer must estimate realistic moment-rotation relationships for the connections. *Design Guide 8* (Leon, Hoffman and Staeger, 1996) provides guidance on the calculation of the connection's rotational stiffness, as does the ASCE Standard 41-13 (ASCE, 2013). An example of the possible influence of the stiffness and strength of the gravity connections is shown in Figure 5, which is taken

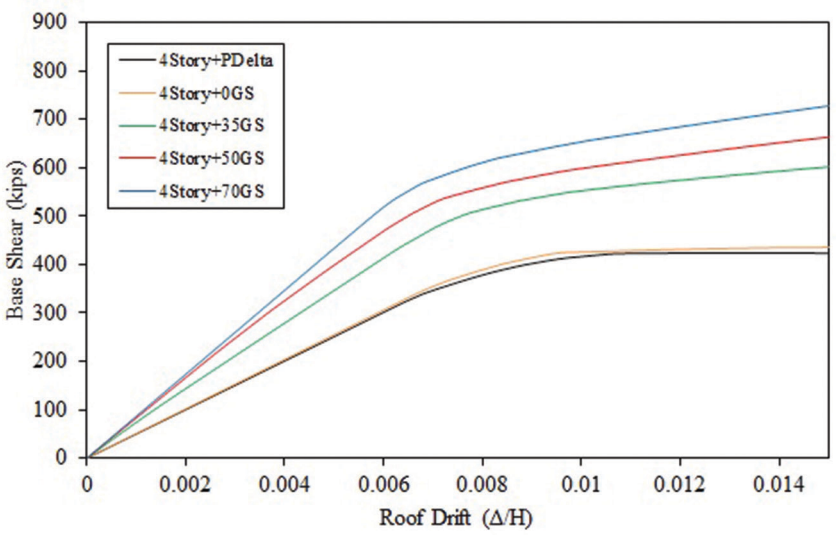

Fig. 5. Nonlinear static pushover curves for a four-story frame.

from analyses of a four-story steel moment frame (Flores and Charney, 2013). The different curves from nonlinear static pushover analysis represent different assumptions regarding the effective strength and stiffness of the connections from the beams to the columns. The curve marked "4Story+PDelta" represents the lateral system only, and the curve marked "4Story+35GS" assumes that the gravity connections have 35% of the stiffness of the full beam section. As may be seen, there is a considerable increase in system stiffness and strength when the gravity system is considered.

While it is recommended that the gravity system be included in the wind serviceability analysis, it is recognized that neglecting the gravity system will be conservative.

Architectural Components

The influence of architectural components on the response of a building under serviceability wind loads depends on the number of components, the location and orientation of the components, the basic in-plane unit stiffness of the component, the method of attachment and the total contributing stiffness of components relative to the overall stiffness of the lateral load-resisting system. In this sense, an infill masonry wall in a three-story building would significantly influence the computed response, but drywall partitions in a 30-story office building would likely provide negligible stiffness. Due to uncertainties in establishing component location and to estimating the component stiffness, it is recommended that architectural components not be included in wind drift serviceability analysis.

Second-Order (P-Δ) Effects

Second-order effects typically increase lateral deflection and should always be included in the model. When modeling second-order effects, a decision must be made concerning gravity loads. Actual live load values are typically much less than design values (Ellingwood and Culver, 1977), making it unreasonable to use design live loads in a serviceability-based P-Δ analysis. It is recommended that unfactored dead loads be used with the mean expected live loads, taken from live load surveys. Table C4-2 of ASCE 7 (2010) contains survey loads for office buildings, residences, hotels and schools.

Foundation

The significance of the flexibility of the foundation on nonstructural deformations depends on several factors, including the composition of the soil and the characteristics of the foundation itself. Consider, for example, the simple structure shown in Figure 6. Here, slight rotation of the mat foundation under the X-braced frame would contribute to the vertical racking in the adjacent bays, as would the axial elongation in the basement columns. Additionally, the P-Δ

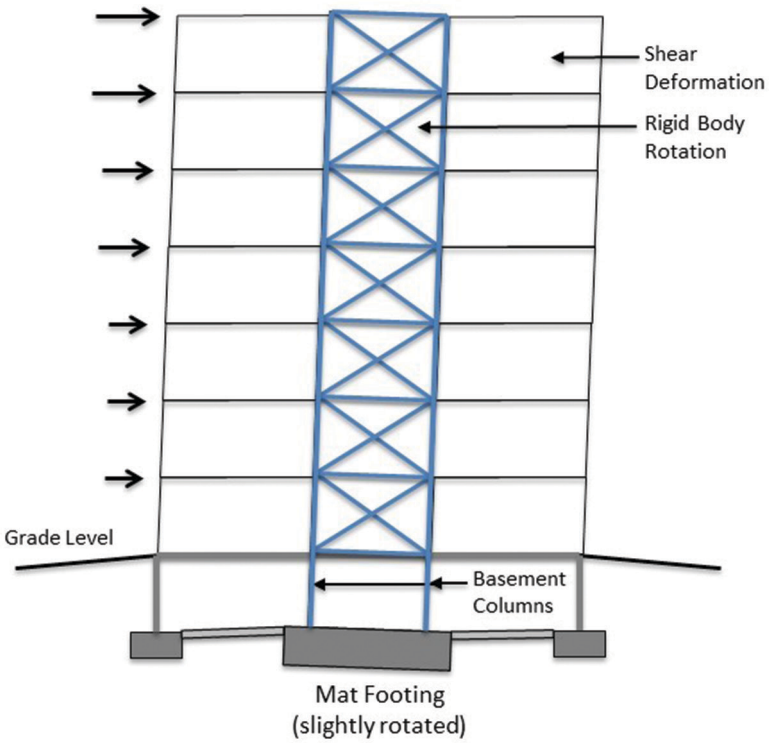

Fig. 6. Foundation modeling concerns.

Table 2. Selected Recommended Shear Strain Limits (Griffis, 1993)			
Building Element	**Supporting Structural Element**	**Deformation Type**	**Recommended Limit**
Brick veneer	Wind frame	Shear strain	*H*/400
Concrete masonry unreinforced (exterior)	Wind frame (1 story)	Shear strain	*H*/600
	Wind frame (2 story)	Shear strain	*H*/400
Concrete masonry reinforced (exterior)	Wind frame (1 story)	Shear strain	*H*/200
	Wind frame (2 story)	Shear strain	*H*/400
Gypsum drywall, plaster	Wind frame	Shear strain	*H*/400
Brick (interior partition)	Wind frame	Shear strain	*H*/1250

effects would be more significant if the foundation and subgrade structure were included in the model. Thus, the shear strains, when used as the EDP, could be significantly underestimated if the mat rotation and the basement columns were not included in the mathematical model.

DAMAGE MEASURES

As already discussed in this paper, the engineering demand parameter (EDP) that is recommended for controlling damage in nonstructural components is shear strain. Such strains develop from the three-dimensional displacements that occur at the attachment points between the structure and the nonstructural component. Given a structural model, the shear strains can be computed with relative ease, either manually or by use of the damage gages described previously.

To control damage, the damage measure (DM) must be compatible with the EDP. Thus, it is logical that those levels of shear strain that cause some level of observable damage in nonstructural components be used as the limiting damage measure. As already mentioned, interstory drift or interstory drift ratios are not suitable as damage measures because they include rigid-body rotations (which do not cause damage) and exclude vertical racking (which does cause damage).

Conventional Drift Limits

Interstory drift limits have historically been based on rules-of-thumb, and ASCE (1988) reported structural engineers to be employing drift limits ranging from $H/600$ to $H/200$, where H is the story height. A review of the literature reveals a commonly suggested interstory drift limit of $H/500$, which is also recommended in *Design Guide 3* (West et al., 2003). However, it should be noted that these limits are generally invariant across material type. Galambos and Ellingwood (1986) provide a broad set of interstory drift limits that are tied to specific serviceability problems that can arise. These limits range from $H/1000$ (cracking of brickwork) to $H/100$ (damage to lightweight partitions, impaired operation of windows and doors, etc.). Within this range, the limit of $H/500$ is associated with the cracking of partition walls. The limits provided by Galambos and Ellingwood, however, are not connected to any specific structural or nonstructural material.

The preceding discussion illustrates the wide range of applied interstory drift limits in historical use. However, these limits are typically not modified by engineers to account for specific structural or nonstructural materials, as limits on shear strain would be. Rather, a designer may indiscriminately employ the same interstory drift limit for each bay in the building, or even for two or more buildings with different owner preferences, functions, and material makeup. For a more accurate measure of component damage, rational shear strain limits intended to control damage to a particular material should be defined on the basis of the material's properties. For example, if the goal is to prevent damage to interior gypsum wall partitions, then the damage limit should be defined based on test data of gypsum wallboard. Using rational damage limits will likely lead to a separate shear strain damage limit for each damageable material in a building.

Griffis (1993) recognized this problem and recommended limiting shear strains in a variety of nonstructural components. Selected values are repeated in Table 2. The recommended limits are those that are expected to be at the threshold of causing observable damage in the given building element and are recommended for use in association with a 10-year MRI. The use of limiting strains as shown in Table 2 is a step in the right direction, but there is no information provided as to the type of damage that could be expected, nor is any information provided as to the likelihood that the damage would occur if the recommended drift limit were to be achieved under the designated wind load.

Fragility

A more rational approach for damage control is based on the concept of *fragility*, specifically, *fragility curves*. A fragility

curve is a mathematical relationship between an engineering demand parameter (e.g., shear strain in nonstructural components) and the probability of attaining some observable damage measure. The curves are based on laboratory test data, usually from a number of sources. Appendix B contains additional information on fragility curve theory. Figure 7 contains three sample fragility curves for gypsum wallboard, obtained from the Performance Assessment Calculation Tool (PACT) developed by the Applied Technology Council (FEMA, 2013b) as a part of FEMA P-58 (FEMA, 2013a). The horizontal axis shows the EDP of deformation damage index (or shear strain), and the vertical axis contains the probability of exceeding one of the three damage states shown. Note that many of the fragilities found in PACT use interstory drift ratio as the EDP. As long as racking tests were performed on the individual component to develop the fragilities, the interstory drift ratio will be equal to shear strain, and therefore, those fragilities can be used in this procedure where the EDP is shear strain. The blue curve in Figure 7 represents damage state 1 (DS1), which is screws popping out and minor cracking. The orange curve (DS2) is DS1 plus moderate cracking or gypsum crushing, and the maroon curve (DS3) is DS2 plus significant cracking or crushing. From Figure 7, it may be seen that for a deformation damage index of 0.005 (1/200) corresponding to a hypothetical 10-year MRI, there is a 7.0% probability of no damage occurring, a 71% probability of the gypsum drywall experiencing DS1, a 19% probability of DS2, and a 2.6% probability of DS3.

One of the advantages of the fragility approach is that a *design space* of information is provided instead of information on just one specific damage limit or wind speed. In this sense, the entire plot represents the design space, and the DDIs that could occur under several MRIs can be examined. In addition to the 10-year MRI previously discussed, Figure 7 also contains vertical lines representing the DDIs under the loads corresponding to the 25- and 50-year wind loads. Note that the location of the wind speed MRI lines will shift laterally on the plot when different geographic locations are chosen. Using this design space, the engineer can gather probabilistic information for a range of MRIs.

Example of 10-Story Frame, Continued

The example of the 10-story frame is now continued to illustrate the use of fragility in the context of engineering demand parameters, damage measures and damage states.

After the MRI is selected, the wind loads are determined, the building is modeled and the DDIs are calculated (see Figure 4), the next step is to select damage limits and then compare the DDIs to these limits. For this example, the deformation damageable zones represent interior gypsum wall partitions with metal studs. It is the owner's preference that there is no greater than a 30% chance of minor damage (DS1) to each partition under the 25-year wind loads.

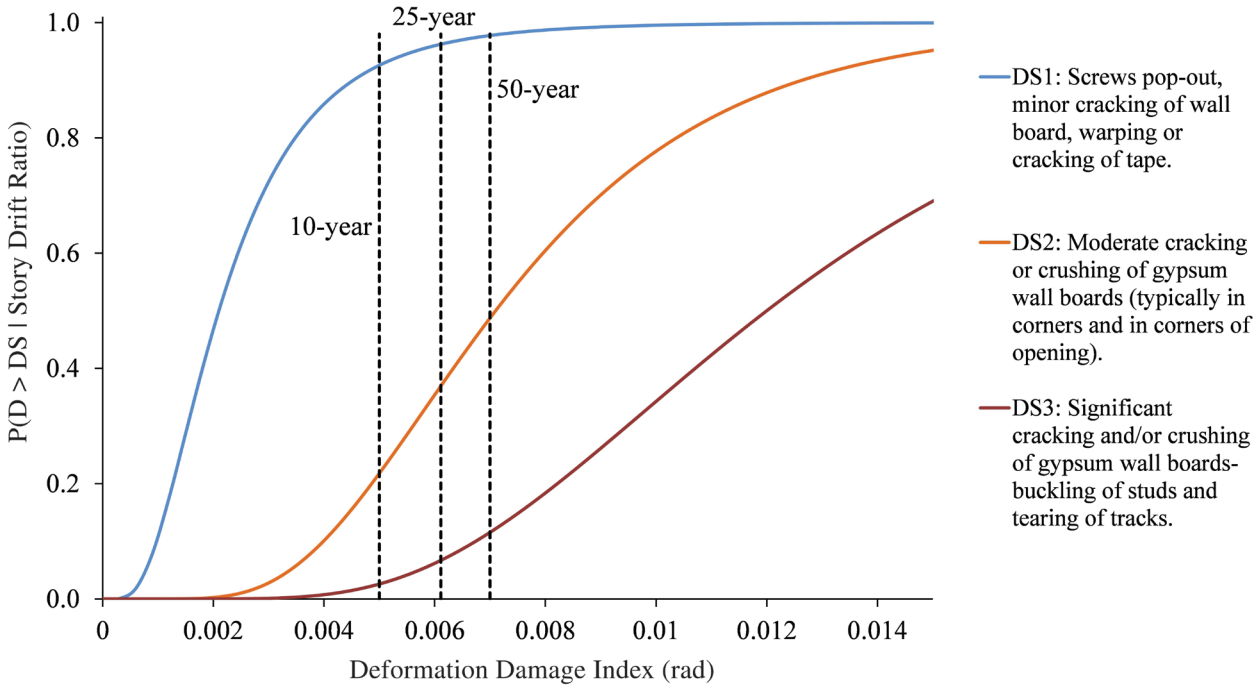

Fig. 7. Gypsum wallboard fragility curves (PACT).

Using the fragility information from Table 5 of Appendix B (median demand = 0.0021, dispersion = 0.6), it is determined that a DDI of 0.00153 corresponds to a probability of exceedance of DS1 of 30%. (See Appendix C for details on computing such probabilities.) Based on the DDIs shown in Figure 4, the outside bays in the top eight levels exceed the limit, while none of the interior (braced) bays do so.

An alternative to comparing the maximum DDI to some limit from the fragility curve is to look at the range of the DDIs in all of the bays of interest. Figure 8 shows the fragility curve for DS1 for gypsum drywall. The middle 50% range of DDIs is shown on the figure, along with the mean of the DDIs for the 10-, 25-, and 50-year wind loads. This figure provides information concerning multiple MRIs. For the 10-year wind loads, the average DDI corresponds to a 10.5% probability of exceeding DS1; for the 25-year MRI, this probability is 18.7%; for the 50-year MRI, it is 26.2%. This constitutes a design space with which the engineer can make a decision based on performance at multiple MRIs.

PERFORMANCE ASSESSMENT AND DECISION MAKING

One of the most challenging aspects of the recommended methodology is making design decisions based on the results of the damage assessment. After the damage assessment has been conducted, the designer must come to a decision concerning the acceptability of the design (either it is adequate or it is not). The decision space (probabilities of damage relative to deformation levels due to various MRIs) aids in this decision-making process, but it is the responsibility of the engineer to set acceptability thresholds (e.g., no more than a 30% probability of exceedance due to the 25-year MRI) in coordination with the architect, building owner and other stakeholders. As discussed later, it will likely be helpful to connect the probability of damage to cost of repair or replacement, thus providing a decision variable in terms of cost, which is typically more useful to a building owner than shear strain or damage probabilities.

OPTIONS FOR REDESIGN IF PERFORMANCE TARGETS ARE NOT MET

In many cases, the designer will find that the structure does not meet the required serviceability requirements and that the system must be re-proportioned to meet such requirements. Unfortunately, it may be difficult to determine which members of the main lateral load-resisting system to modify (make stiffer or more flexible). Virtual work-based procedures (Velivasakas and DeScenza, 1983; Baker, 1990, Charney, 1991, 1993) have been developed to simplify this task and are included in some commercial analysis programs such as SAP2000 (Computers and Structures, 2009), and RAM Frame (Bentley, 2013). These procedures can provide information as to which elements to modify and, even further, to recommend which section properties within these elements (axial area, shear area, moment of inertia) to modify. These simple virtual work methods are the basis of much more complex automated optimization procedures that have been used in tall building design (Chan, Huang and Kwok, 2010).

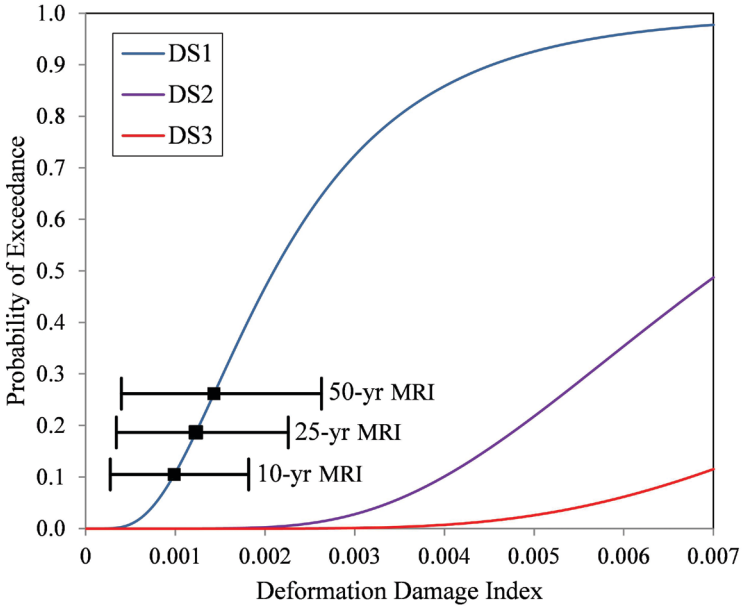

Fig. 8. Middle range of DDIs for the 10-story building.

APPLICATION TO THE FEMA P-58 METHODOLOGY

While the FEMA P-58 (FEMA, 2013a) methodology was developed for seismic response of structures, the procedure and its four goals could easily be adapted to the wind serviceability procedure discussed previously. The FEMA P-58 methodology provides a PBEE framework with four major goals: (1) to include the behavior of nonstructural components; (2) to investigate response at a global level; (3) to relate damages to more meaningful consequences, such as repair time, repair costs, casualties and injuries and potential for unsafe placards; and (4) to account for uncertainties and variations within structural analysis.

The first goal, to include the effects of nonstructural components, is already a crucial part of the wind serviceability procedure presented in this paper, as well as the P-58 procedure. However, the other three P-58 goals could be added to the previous procedure to provide more robust results. The P-58 process gives its final results in terms of the global consequences, using the idea of a building performance model. This model is a collection of information about the structure needed to determine the consequences of a structure under loading. This information includes, among other things, a list of all the structural and nonstructural components in the structure and their potential damage states and consequences. Each individual component will have a set of fragility curves developed for a discrete number of damage states, as discussed previously in this paper. For each of these damage states, the time and cost needed to repair that component under the particular level of damage will be estimated as well.

The wind serviceability procedure developed earlier describes how to relate structural response to component damage through the use of fragility. The FEMA P-58 methodology can be used to take this process one step further and relate the component damages to the global consequences. The P-58 methodology includes hundreds of fragilities for both structural and nonstructural components, as well as their corresponding consequences. By using these fragilities along with their corresponding consequences, the end result will describe the global response and be significantly more meaningful to decision makers because the results will be in terms of repair cost and repair time (time that the structure must be vacated to allow for repair).

This seismic-based methodology could be applied to the wind serviceability procedure because the main input is building information and response. The building information (i.e., shear strains) will be the same regardless of what loads are applied to it, and instead of using the structural response from ground motions, the user could input structural response from wind loads. Traditionally, the P-58 procedure finds the building response under a suite of ground motions and then expands the data using a determined level of dispersion and Monte Carlo simulation (in order to account for variability in seismic analyses). For the wind serviceability procedure, this process could be applied to account for uncertainty in selecting an appropriate serviceability MRI, as discussed earlier. A number of MRIs could be analyzed (e.g., from 10 to 50 years), and a range of possible behaviors could be determined. This range of responses would be converted into potential damages, which will be converted into a distribution of probable consequences.

The P-58 procedure will also be useful if initial targets are not met, as an alternative option to the virtual work methods described in the previous section. When the results are displayed in the corresponding software—the PACT program (FEMA, 2013b)—the consequences are broken down by component. The program determines which components are causing the most problems and have the highest influence on repair cost and time. Along with the global consequences, this methodology could provide valuable information for the engineer to decide which components should be the focus of the redesign.

SUMMARY AND CONCLUSIONS

In this paper, a rational method for the wind serviceability design of steel structures is described. The process includes the calculation of appropriate service loads, accurately modeling all significant sources of deformation and stiffness and the determination of rational shear strain limits based on material test data and fragility curves.

The use of fragility curves combined with an accurate structural model allows the structural engineer more confidence with respect to the building's performance under serviceability level wind loads. Using the recommended procedure, the engineer can estimate probabilities of damage and potentially link these probabilities to cost and repair time, which are meaningful decision variables for owners and decision makers.

The following is a summary of the steps in the procedure recommended in this paper. The proposed method is general and can be adapted for different applications.

1. *Select an appropriate mean recurrence interval.* Various MRIs have been suggested, typically ranging between 10 and 50 years. While the length of the MRI could be adjusted after collaboration with the building owner or decision maker, it is recommended that a basic 25-year wind speed be used as a standard so that the DDIs calculated are generally in the range of the test data used to develop fragility curves for common nonstructural components. Different MRIs may be used for different levels of nonstructural component protection, as appropriate.

2. *Determine wind speed and loading.* The wind speed

corresponding to selected MRIs can be found in ASCE 7-10. Alternatively, there are equations available in the literature to convert between wind speeds associated with a 50-year MRI and wind speeds associated with other MRIs (Peterka and Shahid, 1998). The service wind loads can be determined using the applicable building code.

3. *Accurately model the structure.* The structural model should include all significant sources of deformation and lateral stiffness. The deformation source should include axial, shear, flexural and panel zone deformations, when appropriate. Engineering judgment should be used to determine sources of lateral stiffness to include with the bare frame stiffness. Possible additional lateral stiffness sources include connection flexibility, diaphragm stiffness and gravity frame stiffness. Direct modeling of the soil–foundation interface should also be considered.

4. *Calculate the deformation damage index.* The damage measure for nonstructural components should include vertical racking deformation as well as horizontal racking. For this reason, the DDI should be used instead of the conventional interstory drift index (measuring only horizontal racking). The use of damage gages is recommended because they are easily implemented in most commercial software.

5. *Select rational damage limits.* The deformation damage index should be compared to damage limits that are determined on a rational and consistent basis. In this paper, fragility curves are recommended as the source of information regarding damage to nonstructural components due to shear strain (DDI).

6. *Compare the DDIs with the damage limits.* The calculated DDIs for each bay should be compared with the damage limits determined with fragility curves. Stiffness can be added or subtracted from the structure at locations determined by the engineer.

7. *Repeat steps 1–6 until an economical design is achieved or other loading cases control.*

ACKNOWLEDGMENTS

The authors acknowledge the comments and contributions of the ASCE/SEI Committee on Design of Steel Building Structures. The authors also acknowledge the work of Virginia Tech graduate student Johnn Judd for his work on the wind hazard curves presented in this paper. Funding for authors K. Aswegan and J. Jarrett was partially provided by the Charles E. Via Endowment of the Virginia Tech Department of Civil and Environmental Engineering and by a grant from the National Institute of Standards and Technology (NIST).

SYMBOLS

G	Shear modulus
G_{M25}	Wind gust factor under 25-year MRI
G_{Mx}	Wind gust factor under x-year MRI
H	Interstory height
L	Width of deformation damage zone
K_d	Wind directionality factor (ASCE 7)
K_z	Velocity pressure exposure factor (ASCE 7)
K_{zt}	Topographic factor (ASCE 7)
M	Number of specimens in a set of test data
$P(Z > z)$	Probability of exceedance during time period, T
T	Time period if interest for computing probability of exceedence
V_{M25}	Wind speed under 25-year MRI
V_{Mx}	Wind speed under x-year MRI
X_i	X-coordinate of node i = A, B, C or D of drift damage zone
Y_i	Y-coordinate of node i = A, B, C or D of drift damage zone
i	Rank of sorted set of test data
p_i	Probability of exceedance associated with data point i
q_z	Wind velocity pressure (ASCE 7)
δ_{M25}	Deformation parameter under 25-year MRI
δ_{Mx}	Deformation parameter under x-year MRI
λ	Mean of the natural log of the data set
ξ	Standard deviation of the natural log of the data set (dispersion)

REFERENCES

Applied Technology Council (2013), Wind Speed website, www.atcouncil.org/windspeed.

AISC (2010), *Specification for Structural Steel Buildings,* ANSI/AISC 360-10, American Institute of Steel Construction, Chicago, IL.

Algan, B. (1982), *Drift and Damage Considerations in Earthquake-Resistant Design of Reinforced Concrete Buildings*, PhD Dissertation, Department of Civil Engineering, University of Illinois, Urbana-Champaign, IL.

ASCE (1988), "Wind Drift Design of Steel-framed Buildings: State-of-the-Art Report," *Journal of Structural Engineering*, Vol. 114, No. 9, pp. 2085–2108.

ASCE (2010), *Minimum Design Loads for Buildings and Other Structures*, ASCE 7, American Society of Civil Engineers, Reston, VA.

ASCE (2013), *Seismic Evaluation and Retrofit of Existing Buildings*, ASCE 41, American Society of Civil Engineers, Reston, VA.

Baker, W.D. (1990), "Sizing Techniques for Lateral Systems in Multi-Story Buildings," *Proceedings of the 4th World Congress on Tall Buildings*, Council on Tall Buildings and Urban Habitat, pp. 857–868.

Bentley (2013), www.bentley.com/en-US/Products/RAM+Frame/.

Berding, D.C. (2006), *Wind Drift Design of Steel Framed Buildings: An Analytical Study and a Survey of the Practice*, M.S. Thesis, Department of Civil and Environmental Engineering, Virginia Tech, Blacksburg, VA.

Chan, C.M., Huang, M.F. and Kwok, K.C.S. (2010), "Integrated Wind Load Analysis and Stiffness Optimization of Tall Buildings with 3D Modes," *Engineering Structures*, Vol. 31, pp. 1252–1261.

Charney, F.A. (1990a), "Sources of Elastic Deformation in Laterally Loaded Steel Frame and Tube Structures," *Proceedings of the 4th World Congress on Tall Buildings*, Council on Tall Buildings and Urban Habitat, Bethlehem, PA, pp. 893–915.

Charney, F.A. (1990b), "Wind Drift Serviceability Limit State Design of Multistory Buildings," *Journal of Wind Engineering & Industrial Aerodynamics*, Vol. 36, No. 1–3, pp. 203–212.

Charney, F.A. (1993), "Economy of Steel Framed Buildings through Identification of Structural Behavior," *Proceedings of the Spring 1993 AISC Steel Construction Conference*, Orlando, FL.

Charney, F.A. and Berding, D.C. (2007), "Analysis and Commentary on the Results of a Nationwide State-of-the-Practice Survey on Wind Drift Analysis and Design," *Proceedings of the 2007 Structures Congress*, Long Beach, CA, pp. 1–10.

Charney, F.A. and Marshall, J. (2006), "A Comparison of the Krawinkler and Scissors Models for Including Beam-Column Joint Deformations in the Analysis of Moment-Resisting Steel Frames," *Engineering Journal*, Vol. 43, No. 1, pp. 31–48.

Charney, F.A. and Pathak, R. (2008), "Sources of Elastic Deformation in Steel Frame and Framed-Tube Structures: Part 1: Simplified Subassemblage Models," *Journal of Constructional Steel Research*, Vol. 64, No. 1, pp. 87–100.

Ciampoli, M., Petrine, F. and Augusti, G. (2011), "Performance Based Wind Engineering—Towards a General Procedure," *Structural Safety*, Vol. 33, pp. 367–378.

Committee on Serviceability Research (1986), "Structural Serviceability: A Critical Appraisal and Research Needs," *Journal of Structural Engineering*, Vol. 112, No. 12, pp. 2646–2664.

Computers and Structures Inc. (2009), *SAP2000* (version 14.0.0), CSI, Berkeley, CA.

Dymiotis-Wellington, C. and Vlachaka, C. (2004), "Serviceability Limit State Criteria for the Seismic Assessment of R/C Buildings," *Proceedings of the 13th World Congress on Earthquake Engineering,* Vancouver, BC.

Ellingwood, B.R. and Culver, C.G. (1977), "Analysis of Living Loads in Office Buildings," *Journal of the Structural Division*, Vol. 103, No. 8, pp. 1551–1560.

FEMA (2012), "2009 NEHRP Recommended Seismic Provisions: Design Examples," FEMA P-751, prepared by the Building Seismic Safety Council for FEMA, Washington, DC.

FEMA (2013a), "Seismic Performance Assessment of Buildings: Volume 1—Methodology," FEMA P-58-1, prepared by the Applied Technology Council for FEMA, Washington, DC.

FEMA (2013b), "Seismic Performance Assessment of Buildings: Volume 3—Supporting Electronic Materials and Background Documentation," FEMA P-58-3, prepared by the Applied Technology Council for FEMA, Washington, DC.

Flores, F. and Charney, F.A. (2014), "Influence of Gravity Framing on the Seismic Performance of Steel Moment Frames," *Journal of Constructional Research*, Vol. 101, pp. 351-362.

Galambos, T.V. and Ellingwood, B.R. (1986), "Serviceability Limit States: Deflection," *Journal of Structural Engineering*, Vol. 112, No. 1, pp. 67–84.

Griffis, L.G. (1993), "Serviceability Limit States Under Wind Loads," *Engineering Journal*, Vol. 30, No. 1, pp. 1–16.

Griffis, L.G., Patel, V., Muthukumar, S. and Baldava, S. (2012), "A Framework for Performance-Based Wind Engineering," *Proceedings of the ATC-SEI Advances in Hurricane Engineering Conference*, Miami, FL.

ICC (2012), *ICC Performance Code for Buildings and Facilities*, International Code Council, Washington, DC.

Lee, T., Kato, M., Matsumiya, T., Suita, K. and Nakashima, M. (2006), "Seismic Performance Evaluation of Non-structural Components: Drywall Partitions," *Earthquake Engineering Structural Dynamics*, Vol. 36, No. 3, pp. 367–382.

Leon, R.T., Hoffman, J.J. and Staegar, T. (1996), *AISC Design Guide 8: Partially Restrained Composite Connections*, American Institute of Steel Construction, Chicago, IL.

Microsoft Corporation (2013). *Microsoft Excel*, Microsoft, Redmond, WA.

Miranda, E. and Mosqueda, G. (2013), "Seismic Fragility of Building Interior Cold-Formed Steel Framed Gypsum Partition Walls," *Background Document,* FEMA P-58/BD-3.9.2, Applied Technology Council, Redwood City, CA.

Moehle, J. and Deierlein, G.G. (2004), "A Framework Methodology for Performance-based Earthquake Engineering," *Proceedings of the 13th World Conference on Earthquake Engineering*, Vancouver, CA.

O'Brien, W., Memari, A., Kremer, P. and Behr, R. (2012), "Fragility Curves for Architectural Glass in Stick-Built Glazing Systems," *Earthquake Spectra*, Vol. 2, No. 28, pp. 639–665.

Parametric Technology Corporation (2007). *Mathcad*, PTC, Needham, MA.

Paulotto, C., Ciampoli, M. and Augusti, G. (2004), "Some Proposals for a First Step Towards a Performance Based Wind Engineering," *Proceeding of 1st International Forum in Engineering Decision Making*, Stoos, Switzerland.

PEERC (2010), *Guidelines for Performance-Based Seismic Design of Tall Buildings*. Report 2010/05, November 2010, prepared by the TBI Guidelines Working Group, Pacific Earthquake Engineering Research Center, University of California, Berkeley, CA.

Peterka, J.A. and Shahid, S. (1998), "Design Gust Wind Speeds in the United States," *Journal of Structural Engineering*, Vol. 124, No. 2, pp. 207–214.

Porter, K., Kennedy, R. and Bachman, R. (2007), "Creating Fragility Functions for Performance-based Earthquake Engineering," *Earthquake Spectra*, Vol. 23, No.2, pp. 471–489.

Schaffhausen, R. and Wegmuller, A. (1977), "Multistory Rigid Frames with Composite Girders Under Gravity and Lateral Forces," *Engineering Journal*, 2nd Quarter, pp. 68–77.

Tallin, A. and Ellingwod, B.R. (1984), "Serviceability Limit States: Wind Induced Vibrations," *Journal of Structural Engineering*, Vol. 110, No. 10, pp. 2424–2437.

Vallenilla, C. and Bjorhovde, R. (1985), "Effective Width Criteria for Composite Beams," *Engineering Journal*, 4th Quarter, pp. 169-175.

Velivasakis, E. and DeScenza, R. (1983), "Design Optimization of Lateral Load Resisting Frameworks," *Proceedings of the 8th Conference on Electronic Computation*, American Society of Chemical Engineers, pp. 130–143.

West, M., Fisher, J. and Griffis, L. (2003), *AISC Design Guide 3: Serviceability Design Considerations for Steel Buildings*, American Institute of Steel Construction, Chicago, IL.

APPENDIX A

Example of a 12-Story Perimeter Moment Resisting Frame

In this example, a 12-story, unsymmetrical, steel-framed office building located in Charleston, South Carolina, is analyzed. This building, with slightly different properties, is also used in the Analysis chapter of FEMA P-751 (2012). The first story is 18 ft tall, and the remaining stories are 12.5 ft. The building contains setbacks at levels 5 and 9. At the lower levels of the building, there are seven bays spaced at 30 ft in the east–west direction and seven bays spaced at 25 ft in the north–south direction. The lateral system is composed of perimeter steel moment-resisting frames.

The wind loads are calculated using the ASCE 7 directional procedure (2010). After consultation with the owner of the building, it was determined that a 10-year wind event would be the basis for the serviceability design due to the fact that this is approximately the length of the average tenancy. For completeness, however, results for a 25-year MRI are also provided at the owner's request. The design wind speed of 146 mph and the 10-year MRI serviceability wind speed of 76 mph are determined with the aid of the Applied Technology Council's wind speed calculator. The structure is modeled in SAP2000, and the loads are applied at the nodes. Damage gage elements were added to the exterior corners of the building to represent glazing (glass curtain wall) or drywall and around the interior core (elevator and stairs) to represent ordinary masonry walls or drywall. While the use of drywall on the exterior is not likely for any building, the DDIs computed for these damage gages could be used to represent drywall in unknown or arbitrary locations. Figure A.1 shows two views of the structural model. The vertical shaded elements represent the damage gages located at the perimeter and in the interior of the structure.

Figure A.2 shows the building model with the perimeter DDIs labeled on each damage gage. As expected, the highest DDIs (0.00276, or $1/362$) are found in the first story. Figure A.3a shows the drywall fragilities for DS1 and DS2, together with the maximum DDIs for the 10- and 25-year

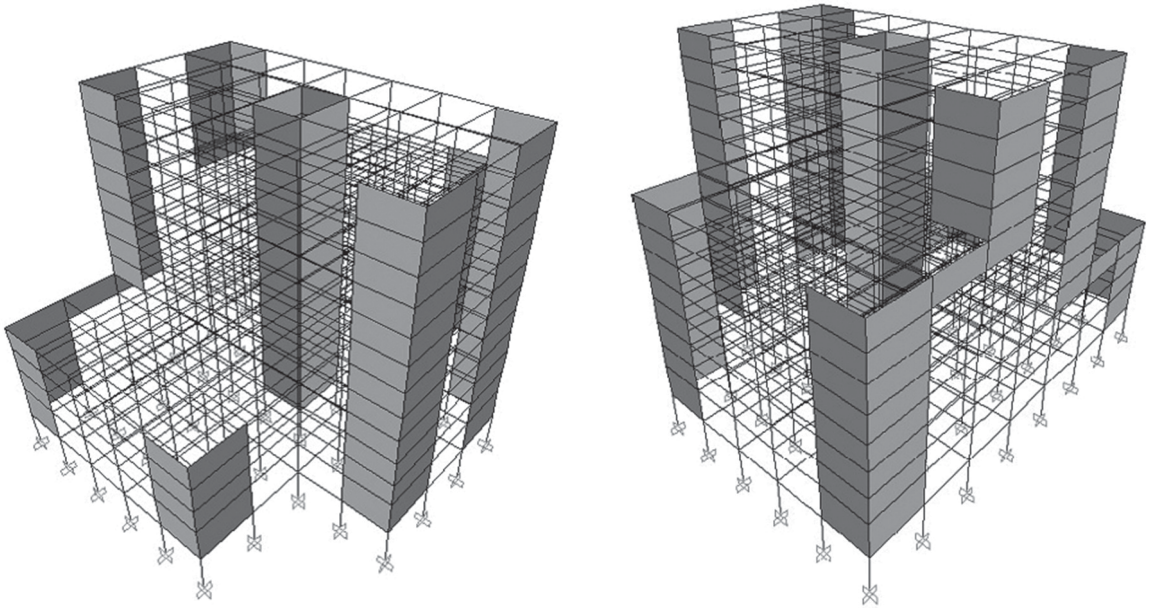

(a) *(b)*

Fig. A.1. Model of 12-story building: (a) from south to west; (b) from north to east.

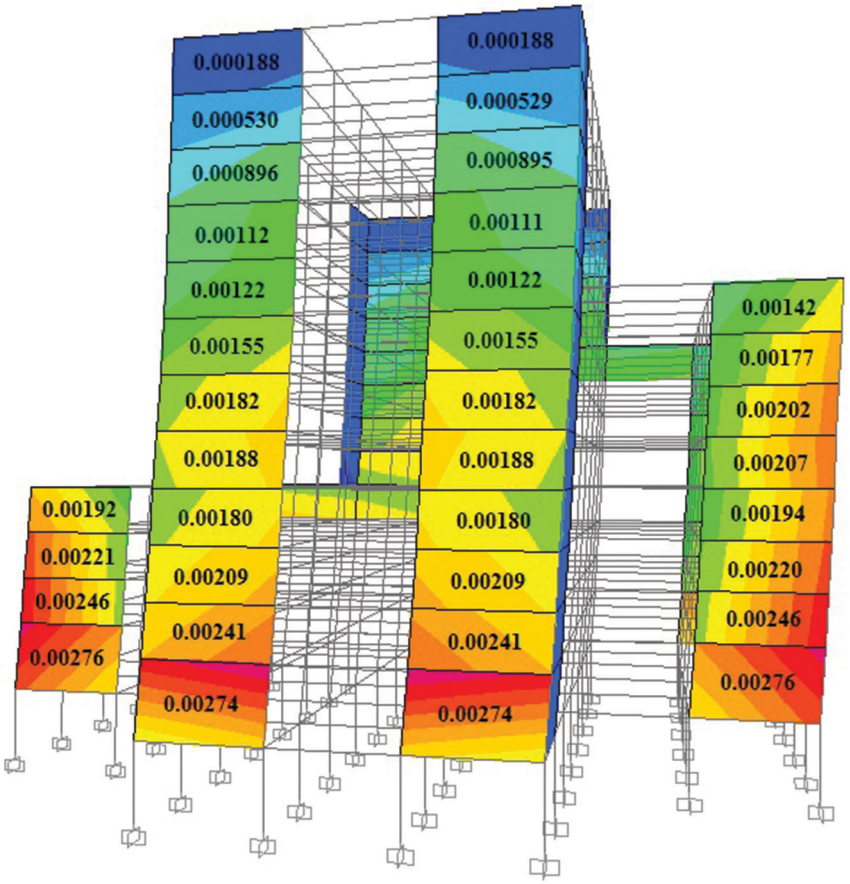

Fig. A.2. Computed DDIs on perimeter of building.

MRIs. There is approximately a 65% probability of exceeding DSI, given the 10-year maximum DDI of 0.00276. Figure A.3b shows the DS1 fragility curve for the glass curtain wall, along with a vertical line at the maximum DDI, computed using the 10-year MRI. The curve illustrates the fact that a DDI of 0.00276 is not an issue for the glass curtain wall because the probability of exceedance of DS1 is negligible.

The interior core masonry walls present a greater issue than the exterior curtain wall. Figure A.4 shows a cross-section of the model under the 10-year wind load with the

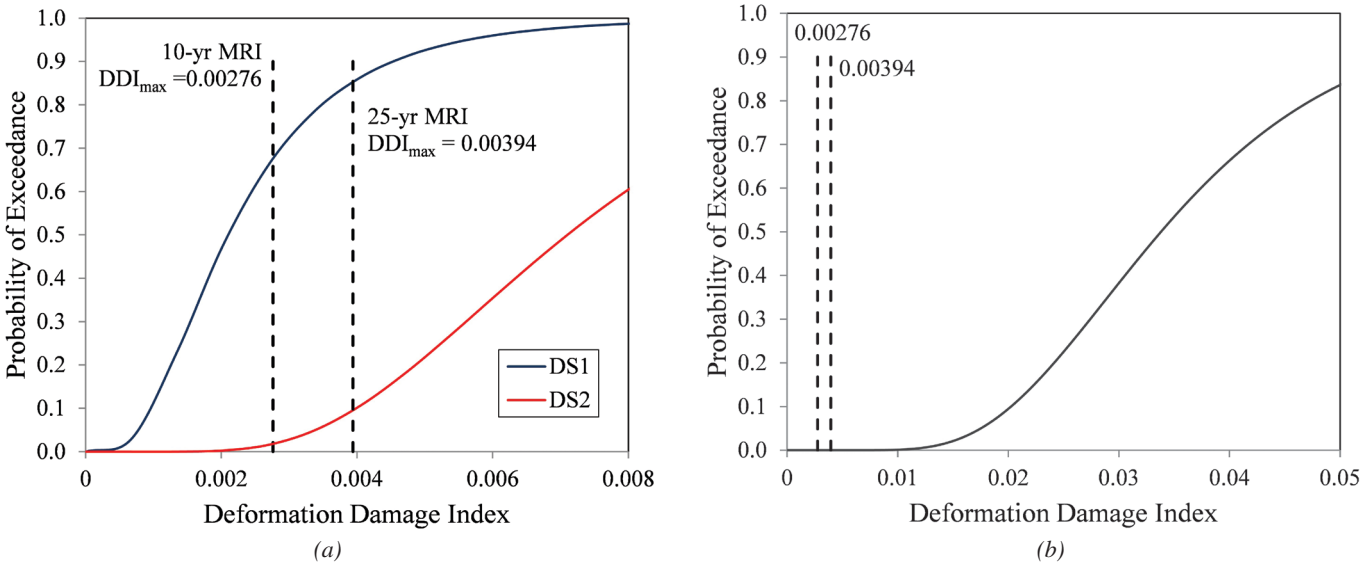

Fig. A.3. Decision spaces for exterior drywall and for exterior curtain wall: (a) drywall; (b) curtain wall for 10-year MRI.

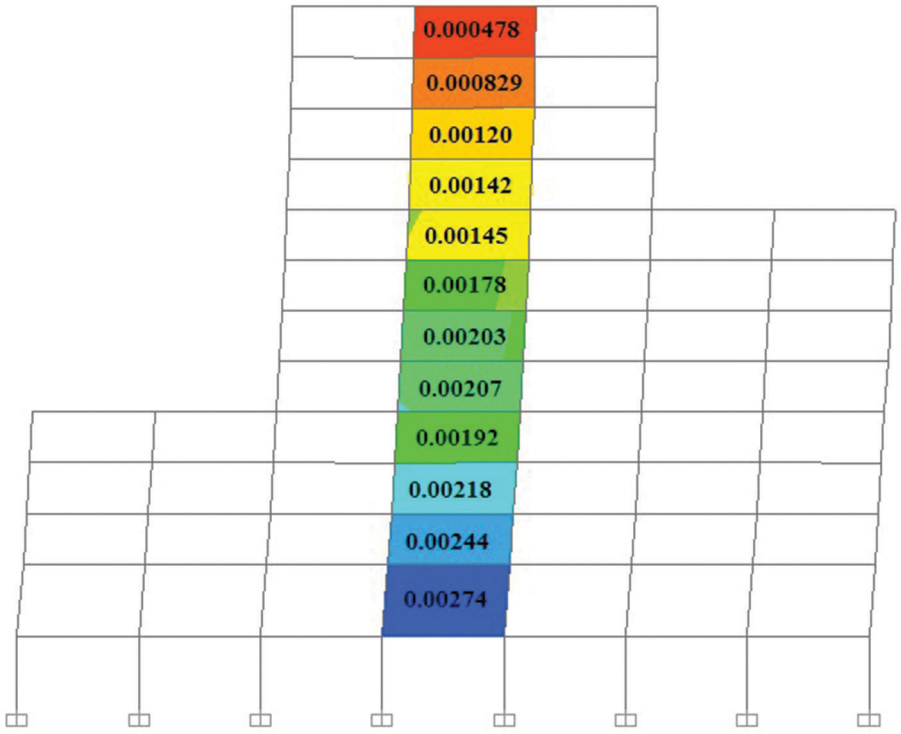

Fig. A.4. Computed 10-year DDIs in core of building.

DDIs for the interior core labeled. The maximum DDI of 0.00274 occurs at the first story, and the minimum of 0.000478 occurs at the top story. Figure A.5a shows two fragility curves for drywall. The minimum, mean, maximum and full range of computed DDI values are illustrated in the figure for the 10-year and 25-year wind loads. Figure A.5b shows the DS1 and DS2 fragility curves for ordinary masonry walls as well as the DDI ranges. The 25-year DDIs were calculated with Equation 1 for a wind speed of 89 mph. The hypothetical building owner has indicated that the average wall in the core (gypsum wallboard or masonry) should have no more than a 30% chance of minor damage (DS1) under the 10-year wind loads and no more than a 70% chance of minor damage under the 25-year wind loads. From Figures A.5a and b, the designer can see that the average DDI (0.00171) under the 10-year wind loads has a probability of exceedance for DS1 greater than 30%, thus failing the owner's requirement. However, the average DDI under the 25-year wind loads is approximately 60%, thus meeting the owner's requirement that it be less than 70%. The DDIs corresponding to other MRIs (such as 50- or 100-year) could also be determined with Equation 1 and incorporated into the decision-making process, provided that the owner has selected an allowable probability of damage corresponding to those MRIs.

A final issue to consider is torsional wind loading. It is prudent to examine the effects of torsional loads, although due to the nature of the lateral load-resisting system (perimeter moment frame) in this building, torsional loading requirements are not likely to control. For this building, torsion was examined according to the provisions of ASCE 7-10, which requires that 75% of the lateral wind load be applied in combination with a torsional moment corresponding to 15% eccentricity. Figure A.6 shows the structure under the 10-year torsional load specified in ASCE 7-10. From Figure A.6, it can be seen that the torsional loading case does not control; the calculated DDIs are lower for this case than for the case in which 100% of the load is applied at no eccentricity (see Figure A.2).

APPENDIX B

Fragility Curve Theory

There are many different methods used to develop fragility curves (FEMA, 2013a; Porter, Kennedy and Bachman, 2007). If the objective of the fragility curve is to obtain rational damage measures, the most useful method is experimental testing. A typical test might involve fixing the base of the component (e.g., a sheet of gypsum wallboard) and applying an in-plane load in order to induce a shear strain. In the ideal testing procedure, there will be no vertical racking and no rigid-body rotation; thus, the shear strain and the interstory drift ratio in the component will be equal. As the test progresses, the load is incrementally increased until a particular damage state is observed (e.g., screws popping out, cracking or crushing). The shear strain at which the damage state occurs is noted, and the test is repeated on a new specimen.

Table B.1 shows data obtained from tests performed on gypsum wall partitions (Miranda and Mosqueda, 2013). The data are collected from six different sources, dating between

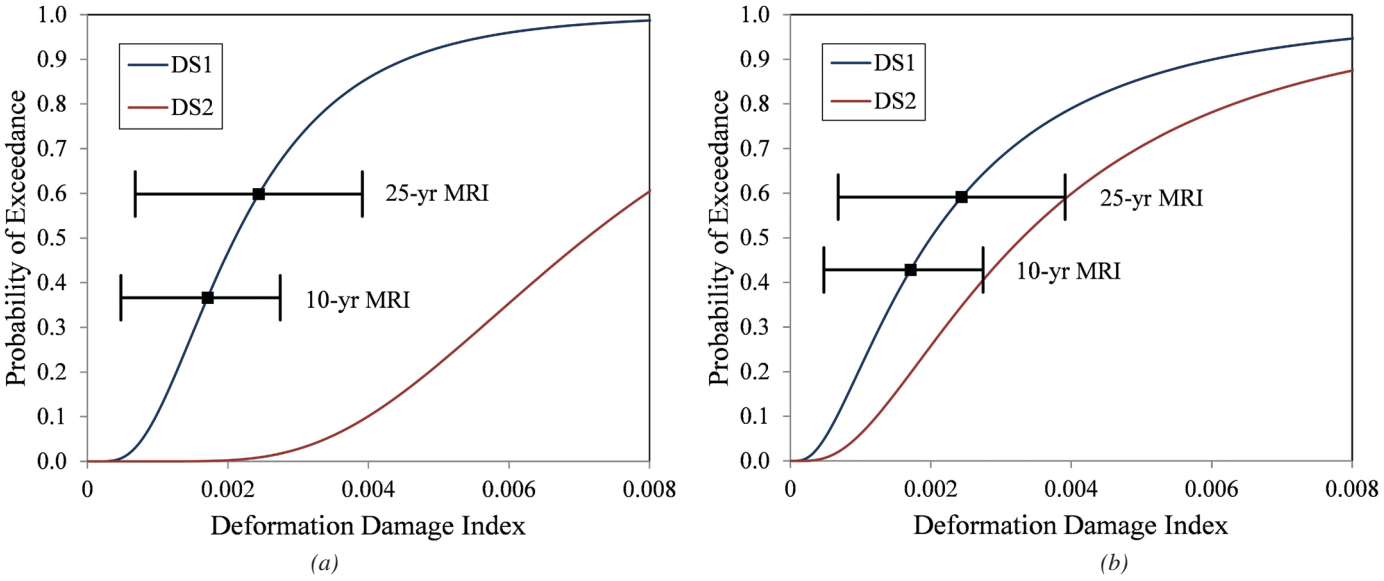

Fig. A.5. Decision spaces for interior drywall and for interior curtain wall: (a) drywall; (b) masonry wall.

Table B.1. Gypsum Partition Wall Data Set (Miranda and Mosqueda, 2013)							
Source	**DS1**	**Source**	**DS1**	**Source**	**DS1**	**Source**	**DS1**
JAB	0.0026	**NEESR**	0.0040	**Rihal**	0.0039	**AMB**	0.0030
	0.0026		0.0020		0.0039		0.0030
	0.0026		0.0040		0.0026		0.0005
	0.0052		0.0020		0.0046		0.0005
	0.0026		0.0040		0.0052		0.0030
	0.0052		0.0020		0.0046		0.0030
	0.0026		0.0020		0.0039		0.0050
	0.0026		0.0040		0.0033		0.0050
	0.0007		0.0040		0.0039		0.0010
	0.0026		0.0040		0.0039		0.0010
	0.0013		0.0040		0.0039		0.0010
	0.0026		0.0040	**Lang**	0.0025		0.0010
Japan	0.0020		0.0040		0.0028		0.0010
							0.0010

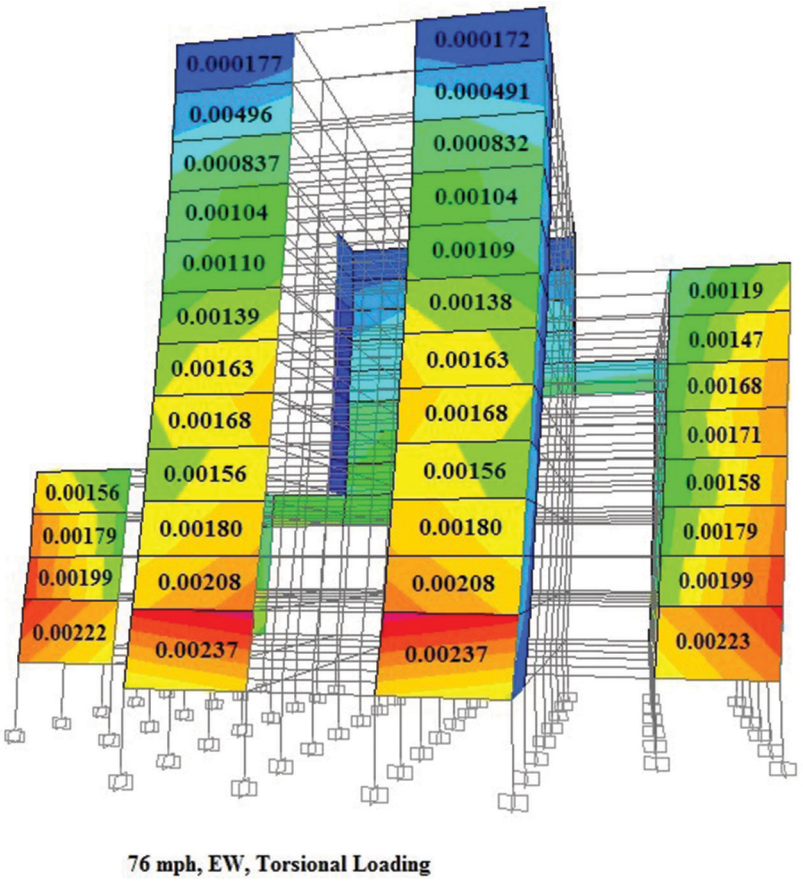

Figure A.6. Computed DDIs on perimeter of building for torsional loading.

Table B.2. Reduced Fragility Data			
(1) Data Point	(2) Sorted Value	(3) Ln(Sorted Value)	(4) Probability
1	0.0005	–7.6	0.0094
2	0.0005	–7.6	0.0283
3	0.0007	–7.264	0.0471
4	0.001	–6.908	0.066
5	0.001	–6.908	0.0948
…	…	…	…
51	0.0052	–5.259	0.9527
52	0.0052	–5.259	0.9716
53	0.0052	–5.259	0.9905
Mean	**0.00297**	**–5.950 = ξ**	—
Standard deviation	**0.00132**	**0.602 = λ**	—

1966 and 2010. The values represent the shear strain (in this case, equivalent to the interstory drift ratio due to the absence of vertical deformation) at which damage state 1 (minor damage such as cracking of drywall or warping of tape) was first observed.

The "raw" fragility data are plotted as solid symbols in Figure B.1. Such a plot is created by first sorting the fragility data in ascending order and then assigning a probability to each data point as follows:

$$p_i = \frac{i - 0.5}{M} \tag{B.1}$$

where M is the number of sample points and i is the rank of the sorted data point.

Table B.2 shows some of the data from Table B.1 that are used to plot the symbols in Figure B.1, where column (2) of the table provides the X-axis values, and column (4) of the table provides the Y-axis values.

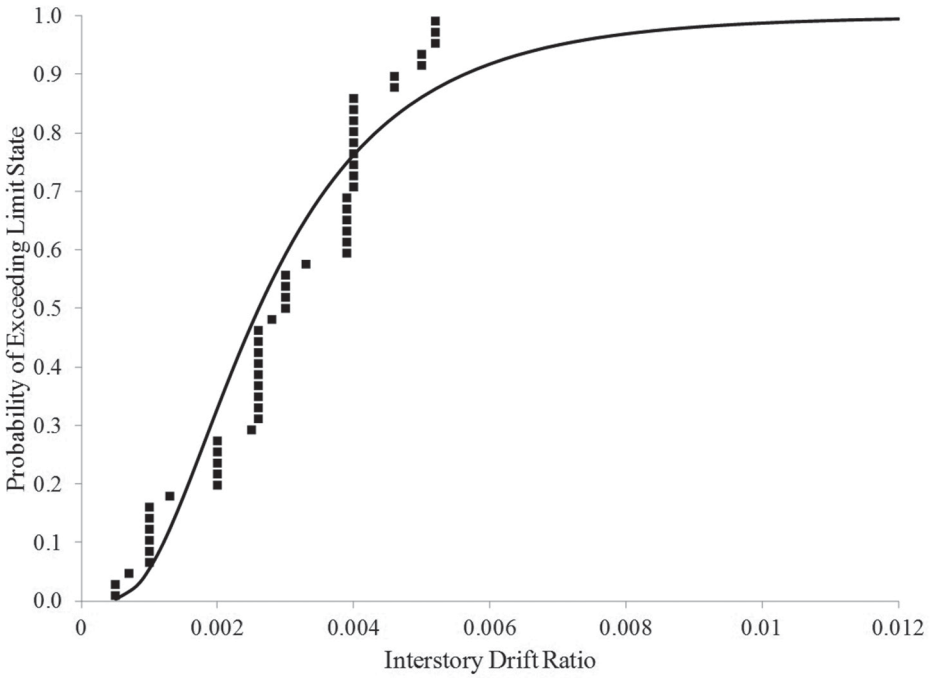

Fig. B.1. Fragility curve construction.

Table B.3. Fragility Information for Gypsum Drywall Building Elements (PACT)				
Building Element[1,2,3]	**Damage State**	**Mean Demand**	**λ**	**Dispersion (ξ)**
Fixed below, fixed above	DS1	0.0021	–6.166	0.60
	DS2	0.0071	–4.948	0.45
Fixed below, slip track above with returns	DS1	0.002	–6.215	0.70
	DS2	0.0050	–5.298	0.40
Fixed below, slip track above without returns	DS1	0.0035	–5.655	0.70
	DS2	0.0093	–4.678	0.45

Notes:
1. DS1 is screw pop-out, minor cracking of wallboard, warping or cracking of tape. DS2 corresponds to moderate cracking or crushing.
2. Full height wall with gypsum on metal studs.
3. These fragilities also apply to gypsum plus wallpaper, gypsum plus ceramic tile and high-end marble or wood panel, provided that the fixities (below and above) are equivalent. See PACT for more information.

Table B.4. Fragility Information for Exterior Enclosure Building Elements (PACT)				
Building Element	**Damage State**	**Mean Demand**	**λ**	**Dispersion (ξ)**
Glass curtain wall (monolithic)[1]	DS1	0.0338	–3.387	0.40
	DS2	0.0383	–3.262	0.40
Glass curtain wall (insulating glass units)[1]	DS1	0.021	–3.863	0.45
	DS2	0.024	–3.730	0.45
Generic storefront (monolithic)[2]	DS1	0.029	–3.540	0.50
	DS2	0.0473	–3.051	0.25
Generic storefront (insulating glass units)[2]	DS1	0.059	–2.830	0.25
	DS2	0.0665	–2.711	0.35

Notes:
1. Generic midrise stick-built curtain wall. Aspect ratio = 6:5. DS1 corresponds to glass cracking. DS2 corresponds to glass falling from frame. For fragility information relating to other glass types, aspect ratios and installation details, see PACT.
2. Aspect ratio 6:5. DS1 corresponds to a gasket seal failure. DS2 corresponds to glass cracking.

The mathematical fragility curve is simply the integral of a probability distribution function (PDF). In most cases, a lognormal PDF is used, as follows:

$$f_X(x) = \frac{1}{(x\zeta)\sqrt{2\pi}} \exp\left[-\frac{1}{2}\left(\frac{\ln x - \lambda}{\zeta}\right)^2\right] x \geq 0 \quad \text{(B.2)}$$

where λ is the mean of the natural log of the set (ln x) and ξ is the standard deviation of the natural log of the data set. For example, for the gypsum partition wall data shown in Table B.1, λ = –5.95 and ξ = 0.602. These values are computed as shown in column (3) of Table B.2.

The smooth mathematical fragility function is given by:

$$P(X \leq x) = \int_0^x f_X(x)\,dx \quad \text{(B.3)}$$

The fitted curve in Figure B.1 represents the mathematical fragility function given by Equation B.3.

Note that before using a curve developed from test data for design purposes, a goodness-of-fit test should also be performed (Porter et al., 2007). Additional caution should be exercised when using shear strains that correspond to sections of a fragility curve where there is little data resolution. To avoid this problem, it may be appropriate to select an MRI such that the corresponding shear strains from the fragility curve fall within a segment of the curve with a high resolution of tested data points.

Tables B.3 through B.6 contain λ values (mean of the natural log of the data), dispersion ξ values (standard deviation of the natural log of the data) and the descriptions of the associated damage states for a variety of nonstructural and structural components. The values in the tables were taken from the Performance Assessment Calculation Tool (FEMA, 2013b), which contains the same type of information for hundreds of structural and nonstructural components. PACT also contains useful data on the cost of repairing or replacing the building elements. When the cost data are combined with the probability of damage occurring,

Table B.5. Fragility Information for Concrete and Masonry Building Elements (PACT)				
Building Element	**Damage State**	**Mean Demand**	**λ**	**Dispersion (ξ)**
Reinforced concrete wall (low aspect ratio)[1]	DS1	0.0055	–5.203	0.36
	DS2	0.0109	–4.519	0.30
Low-rise reinforced concrete wall[2]	DS1	0.0076	–4.880	0.35
	DS2	0.0134	–4.313	0.45
Slender concrete wall[3]	DS1	0.0076	–4.880	0.35
	DS2	0.0134	–4.313	0.45
Ordinary reinforced masonry walls[4]	DS1	0.002	–6.215	0.86
	DS2	0.0033	–5.714	0.77
Special reinforced masonry walls[5]	DS1	0.0036	–5.627	0.59
	DS2	0.0059	–5.133	0.51

Notes:
1. DS1 corresponds to cracks of width between 0.04 and 0.12 in. DS2 represents crushed concrete core, localized concrete cracking (width > 0.12 in.) and buckling of vertical rebar.
2. Wall with return flanges. DS1 is crushed concrete core, localized concrete cracking (widths > 0.12 in.) and buckling of vertical rebar. DS2 is sliding of the wall resulting in distributed cracking.
3. DS1 corresponds to spalling of cover and vertical cracks. DS2 is exposed longitudinal reinforcing and buckling of vertical rebar. DS2 is sliding of the wall resulting in distributed cracking.
4. Partially grouted cells, shear dominated. DS1 is first occurrence of major diagonal cracks. DS2 is wide diagonal cracks in each direction, crushing or spalling at wall toes.
5. Fully grouted cells, shear dominated. DS1 is first occurrence of major diagonal cracks. DS2 is wide diagonal cracks in each direction, crushing or spalling at wall toes.

Table B.6. Fragility Information for Structural Steel Building Elements (PACT)				
Building Element	**Damage State**	**Mean Demand**	**λ**	**Dispersion (ξ)**
Braced frame (no seismic detailing)[1]	DS1	0.0042	–5.473	0.25
Ordinary steel concentric braced frame[2]	DS1	0.00159	–6.444	0.70
	DS2	0.010	–4.605	0.30
Special steel concentric braced frame[3]	DS1	0.0035	–5.655	0.46
	DS2	0.0058	–5.150	0.65

Notes:
1. Design for factored loads, no additional seismic detailing. DS1 corresponds to the fracture of brace or gusset plate, gusset buckling and significant decrease in lateral stiffness.
2. DS1 is minor damage, including some buckling of the brace and initial yielding of the gusset. DS2 is moderate damage, including additional brace buckling, gusset yielding and yielding of members.
3. WF braces, balanced design criteria. DS1 corresponds to initial brace buckling, yielding of the gusset and slight residual drift. DS2 is moderate damage, significant buckling of brace, initiation of yielding and out-of-plane deformation of the gusset, initiation of cracking of welds of gusset and yielding of members.

the engineer can estimate an expected repair cost over the time period in question. This aspect of the serviceability design is discussed later with regard to the potential adaptation and application of PACT to PBWE. More information on component testing and fragility development for specific components can be found in Miranda and Mosqueda (2013), Lee et al. (2006), O'Brien et al. (2012), and Algan (1982). Additionally, if the fragility parameters for a particular component cannot be found, fragility curves can be developed by the engineer, using the FEMA P-58 Appendix H procedures (FEMA, 2013a). If actual test data are available, the engineer should use the mean and dispersion (appropriately adjusted for testing procedures) to create a fragility curve. In the absence of test data, other procedures may be used, including Monte Carlo simulation, "expert opinion" and the "single calculation" procedure, which consists of determining a best estimate for the average capacity (Q) of the component and setting the mean value equal to $0.92Q$, with a dispersion equal to 0.40. This procedure can be applied when damage state means are known, but dispersions are unknown or difficult to quantify.

APPENDIX C

Creating Fragility Curves with Software Programs

Although the Performance Assessment Calculation Tool (PACT) can be used to create and view fragility curves, the engineer may wish to create and manipulate the curves with the use of commercial software such as Microsoft Excel, Mathcad, or some other program. Many software programs contain built-in functions capable of producing fragility curves through the use of lognormal distribution functions.

In Microsoft Excel (Microsoft Corporation, 2013) the fragility curve can be plotted using the **lognorm.dist** function. This function takes the following form: **lognorm.dist(*x*, mean, dispersion, cumulative)**, where x is the engineering demand parameter at which the probability of exceedance is to be evaluated, mean is λ, dispersion is ξ and cumulative is true or false (if true, the cumulative distribution function is returned; if false, the probability density function is returned). Referring to the 10-story example, it was determined that a DDI of 0.00153 represents a 30% probability of exceedance of DS1 (mean demand = 0.0021, dispersion = 0.6). This can be calculated using **lognorm.dist(0.00153, ln(0.0021), 0.6, TRUE) = 0.30**.

In Mathcad (Parametric Technology Corporation, 2007) the fragility curve is created with the **plnorm** function, of the form **plnorm(*x*, mean, dispersion),** where the required inputs are defined in the same manner as the Excel function.

ABBREVIATIONS

DDI	deformation damage index
DDZ	deformation damageable zone
DG	damage gage
DM	damage measure
DS	damage state
EDP	engineering demand parameter
IDI	interstory drift index
MRI	mean recurrence interval
PACT	performance Assessment Calculation Tool
PBEE	performance-based earthquake engineering
PBWE	performance-based wind engineering